Table 1. **Effect of bead agitation on hybridization signal intensities with the new DNA chip.** The target DNA originated from the pKF3 plasmid.

Concentration of DNA (ng/μl)	0.15	0.3	0.75
With agitation	2,020	2,470	4,510
Without agitation	660	770	1,400
Ratio of (with agitation)/ (without agitation)	3.1	3.2	3.2

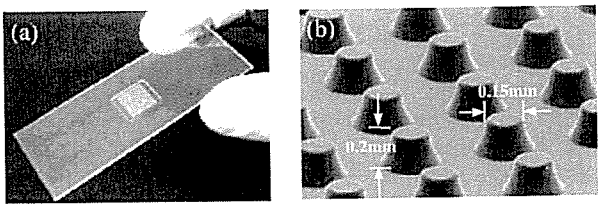

Fig. 1. **(a) Photograph of the new DNA chip and (b) magnified SEM image of pillars at the center of the substrate.**

chip substrate is manufactured by injection molding. Figure 1 (a and b) shows a photograph and a SEM image of this chip substrate, respectively. The oligonucleotides were covalently immobilized on the upper surface of the pillars according to the following procedure.

Surface treatment and oligonucleotide immobilization: The side chain of PMMA was hydrolyzed in an aqueous 1 N sodium hydroxide solution to produce carboxyl groups on the surface. 5′-Amino–modified oligonucleotides, dissolved in an aqueous solution at 30 μM, were spotted onto the upper surface of the pillars robotically using Gene STAMP II (Nippon Laser & Electronics Lab.). The solution ("spotting solution") comprised 100 mM 2-morpholinoethanesulfonic acid, pH 7.0 (MES, Sigma), 500 mM NaCl, 50 mg/ml 1-ethyl-3-(3-dimethylaminopropyl) carbodiimide (EDC, Dojindo), and 0.005% (w/v) sodium dodecylsulfate (SDS, Sigma). After spotting, the substrate was incubated for 16 h in a 100% humidity chamber at 37°C and then washed with Milli-Q water. The oligonucleotides were immobilized the entire tops of the pillars through amide bonds. Figure 7b shows the reaction scheme.

Reference DNA Chip—Reference DNA chips were fabricated using commercially available glass slides (SDA0011; Matsunami Glass Industries, Ltd.). The 5′-amino–modified oligonucleotides described above were dissolved in Solution-I (Takara-Bio) at 30 μM and then spotted robotically. After spotting, the glass slides were incubated for 16 h in a humid chamber and then immersed for 20 min in a blocking solution (DBL0500; Matsunami Glass Industries, Ltd.). The glass slides were washed twice with Milli-Q water and once with ethanol, and then dried.

Target DNAs—In most experiments, target DNAs were prepared as described below: Total RNAs extracted from human brain and liver were purchased from BD Biosciences Clontech. Cy3 (Brain)- and Cy5 (liver)-labeled cDNAs were synthesized by reverse transcription from total RNAs using a CyScribe First-Strand cDNA Labeling Kit (RPN6200; Amersham Biosciences), according to the manufacturer's instructions.

In some experiments (Fig. 7), a chemically synthesized 20-mer oligonucleotide (sequence, 5′-CTTGTCGATCAAGTTCTCCA; Cy3-labeled at 5′-terminal) was used. A labeled DNA originating from pKF3 was also used in place of the target DNA (Table 1 and Fig. 8). The latter was prepared as follows: A pKF3 template was amplified by PCR (primer sequences: 5′-GGGCGAAGAAGTTGTCCATA-3′ and 5′-GCAGAGCGAGGTATGTAGGC-3′). The PCR conditions were as follows: initial 94°C for 4 min, and them 94°C for 40 s, 59°C for 1 min, 72°C for 1 min; 35 cycles. All PCR experiments were conducted with PCT-200 (MJ Research). The PCR products were purified by ethanol precipitation, dissolved in 40 μl of water and then heat-denatured. Next, 2 μl of a random 9 bases primer (6 mg/ml), 5 μl of 10× Klenow buffer, 2.5 μl of a dNTP mixture (2.5 mM each dATP, dTTP and dGTP, and 400 μM dCTP), 2 μl of Cy3-dCTP (Amersham Bioscience), and 10 U of Klenow fragment (2140A; Takara Bio) were added to the DNA solution. The mixture was incubated for 4 h at 37°C and the labeled product was purified by ethanol precipitation.

Hybridization—For the new DNA chip, we devised a special hybridization method to enhance the hybridization fluorescence signal. Briefly, a 20 × 20 mm transparent plastic cover with two through-holes, 0.8 mm in diameter and at opposite corners, was bonded to the center portion of the substrate with double-coated adhesive tape (No. 532; Nitto Denko Co., Ltd.). Figure 2 shows illustrations of the new DNA chip. The target DNA was dissolved in 40 μl of hybridization solution; this solution was applied to the center of the new DNA chip through the holes using a micropipette. About 0.5 mg of micro-glass beads, 125 μm in diameter, suspended in the hybridization solution, was also applied to the center of the new DNA chip in the same way. The hybridization solution comprised 5× SSC (saline-sodium-citrate; Sigma), 0.1% (w/v) SDS, 1% (w/v) BSA (bovine serum albumin; Sigma), and 0.01% (w/v) salmon sperm DNA (Sigma). The holes were sealed with adhesive tape. Beads added to the hybridization solution were driven between the convex-concave structures of the new DNA chip, which agitated the hybridization solution. The beads moved in the concave portion of the new DNA chip without scratching the upper surface of the pillars whereon the oligonucleotides were immobilized.

For reference DNA chips, the target DNA was dissolved in 30 μl of hybridization solution. A 50 × 20 mm cover glass (CG00014; Matsunami Glass Industries, Ltd.) was placed on the spotted area of the slide glass, and then the target DNA solution was applied.

Both the new and reference DNA chips were incubated for 16 h at 42°C. For the new DNA chip, the hybridization solution was agitated by movement of the beads during the hybridization. After the hybridization, the covers were removed, and the chips were washed with 3× SSC containing 0.1% SDS, 1× SSC and 0.1× SSC sequentially at room temperature, and then dried with a spin drier. Hybridization signals were scanned using a DNA chip scanner (GenePix 4000B; Axon Instruments).

Quantitative Real-Time PCR Analysis—Real-time RT-PCR (TaqMan) analysis was carried out using an ABI Prism 7000 Sequence Detector System (Applied Biosystems), according to the manufacturer's instruction. TaqMan probes (Assay-on-Demand) were purchased from Applied Biosystems.

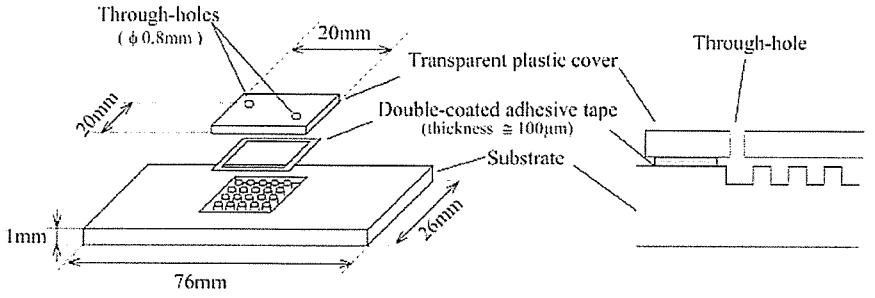

Fig. 2. **Schematic illustrations of the new DNA chip; the right one shows a side view of the chip.**

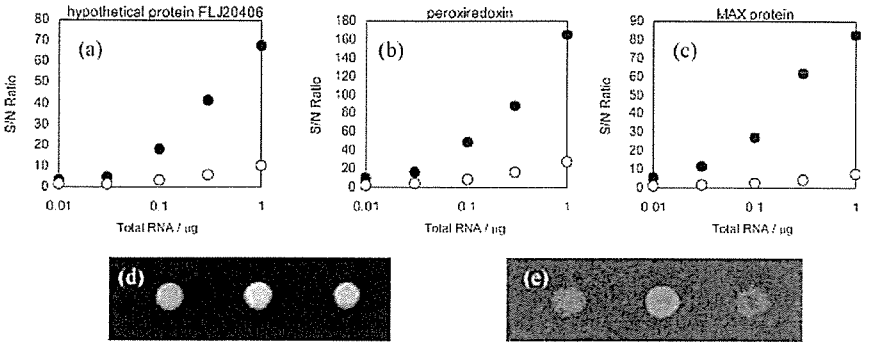

Fig. 3. **S/N ratios and fluorescence images of the new and reference DNA chips after hybridization.** The S/N ratios for the new (solid circles) and reference (open circles) DNA chips for three selected genes are shown in (a), (b) and (c). Fluorescence images of the new (d) and reference (e) DNA chips (amount of total RNA, 0.1 μg) are also shown. In each image, the spots represent hypothetical protein FLJ20406, peroxiredoxin and MAX protein from the left.

Table 2. **Signal intensities obtained with the new and reference DNA chips (amount of total RNA, 0.1 μg).**

Gene name	Serine/ threonine kinase 24	Peroxiredoxin	MAX protein
Signal intensity of new DNA chip	1,070	4,010	2,220
Signal intensity of reference DNA chip	510	1,500	520
Ratio of (new DNA chip)/ (reference DNA chip)	2.1	2.7	4.3

RESULTS AND DISCUSSION

We first examined the agitation effect on the hybridization efficiency using the new chip. Table 1 shows the concentration dependence of the hybridization efficiency with and without agitation of the solution by beads.

The hybridization signals in both cases decreased with decreasing concentration of the target DNA. This result indicates that the agitation with the beads increased the hybridization signals to more than three times compared with no agitation. In the case of no agitation, the low signal intensity was due to the low diffusion constant (D) of the target DNA in the solution. The diffusion constant of 25 bases oligonucleotides is reported to be 8×10^{-8} cm^2/s (*20*). Therefore, the mean square distance of the target DNA in 16 h is calculated to be 0.0092 cm^2, and the average migration distance is 0.096 cm. This average migration distance indicates that only a 1.5% of the target DNA in the hybridization solution is accessible to the probe DNAs on the pillars without agitation under our conditions, assuming the area of hybridization assay is 4 cm^2.

In the next step, the signal intensities obtained with the new DNA chip were compared with those obtained with the reference DNA chip. Three oligonucleotides were selected from the commercially available oligonucleotide set (hypothetical protein FLJ20406, peroxiredoxin and MAX protein). After synthesizing a Cy3-labeled cDNA from 5 μg of total RNA, 0.1 μg of cDNA was applied to the new DNA chip as well as to the reference DNA chip. As shown in Table 2, the new DNA chip showed a markedly higher signal intensity sensitivity, approximately 2–4 times fold higher, than the reference DNA chip.

Next, we examined the signal-to-noise (S/N) ratio of the new DNA chip compared with that of the reference DNA chip because not only enhancement of the signal but also control of the background noise is important for the development of new DNA chip. In most cases, the noise mainly comes from nonspecific adsorption of target DNA onto the substrate. Figure 3 (a, b and c) shows the S/N values obtained with three kinds of target DNA. The results indicate that the new DNA chip showed a markedly higher S/N ratio, approximately 20–100 fold higher, than the reference DNA chip. That is to say, the new DNA chip required small amounts of target DNA (1/20–1/100) to show an equivalent S/N ratio to in the case of the reference DNA chip.

Figure 3 (d and e) shows fluorescence images of the new and reference DNA chips after hybridization. These images clearly indicate the new DNA chip gives higher signals and lower noise compared to the reference chip. In the case of Fig. 3 (d and e), the S/N ratio for the new DNA chip was approximately 5–10 fold higher than that for the reference DNA chip. The high S/N ratios of the new DNA chip were obtained by enhancing the signal level as well as by reducing the noise level. In the case of the new DNA chip, the

noise level was 60–70% lower than that for the reference DNA chip (data not shown). The enhanced signal level was predominantly due to the bead agitation. The markedly reduced noise was due to three reasons. The first reason is the new chip's unique structure. Table 3 shows the relationship between defocus and noise intensity on untreated substrates. As we expected, the noise decreases in the background area when the focal point is adjusted to the top of the pillar. Practically, the noise decreased to 60% when the defocus distance was 200 μm. The second reason is that PMMA exhibits low autofluorescence. Table 3 shows the comparison of the noise of due to PMMA and the slide glass used for the DNA chips. The noise mainly comes from the autofluorescence of the substrates. The noise of PMMA is less than that of the glass substrate. The last reason is surface charges on the substrate. Unreacted carboxyl groups might remain on the surface after the reaction, as shown Fig. 7. Because the carboxyl group shows negative charge at neutral conditions, repulsive forces might exist between the negatively charged target DNA and the surface, resulting in less nonspecific adsorption of the target DNA during the hybridization assay.

Table 3. **Relationship between defocus and the noise level on untreated substrates.**

Defocus (μm)	0	50	100	200
PMMA substrate	330	250	190	180
Glass slide (SDA0011)	460	–	–	–

Next, we investigated whether our DNA chip is applicable to gene expression analysis with a small amount of target DNA. Cy3- and Cy5-labeled cDNAs synthesized from the total RNA (1 to 0.01 μg) from human brain and liver, respectively, were used as target cDNAs. Fluorescence images of the new and reference DNA chips after hybridization are shown in Fig. 4. As shown in Fig. 4, all the hybridization signals obtained using the new DNA chip were markedly higher and had lower noise compared to with the reference DNA chip. In particular, when the amount of total RNA was 0.1 or 0.01 μg, most signals were difficult to detect for the reference DNA chip, while signals on most spots were clearly observed with the new DNA chip. Figure 5 shows scatter plots of the new and reference DNA chips with different amounts of total RNA. The new DNA chip showed a wide dynamic range even when the amount of total RNA was 0.1 or 0.01 μg.

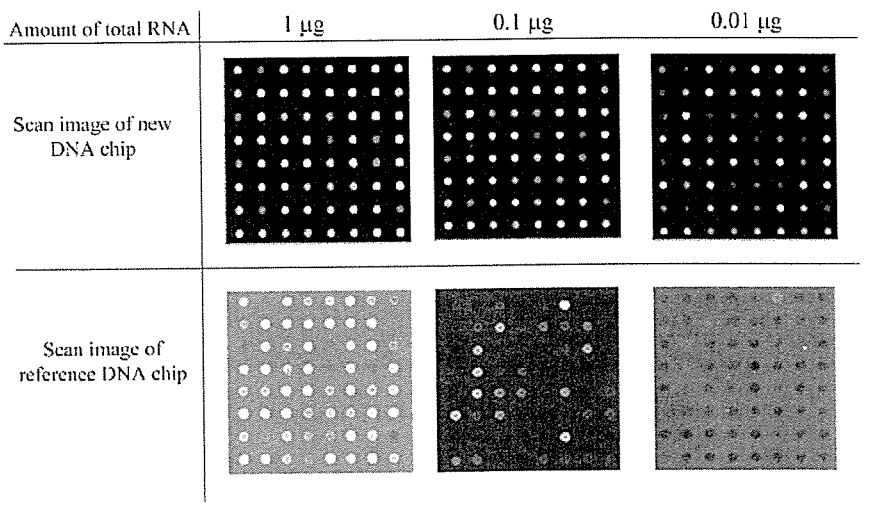

Fig. 4. **Scan images of the new and reference DNA chips.**

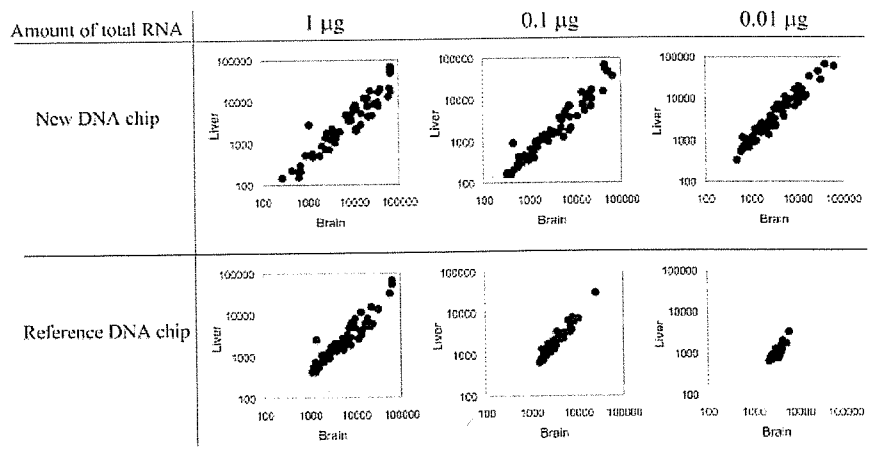

Fig. 5. **Scatter plots of the new and reference DNA chips with different amounts of total RNA.**

On the other hand, the dynamic range of the reference DNA chip became narrower as the amount of total RNA decreased. In the next step, we examined the Cy3/Cy5 ratio to confirm the reliability of the new DNA chip. The analysis was performed with different amounts of total RNA (1 and 0.1 μg, 1 and 0.01 μg). The correlation coefficients obtained with using the new and reference chips are summarized in Table 4. The values for the new chip are obviously superior to those for the reference chip. In particular, the correlation coefficient for the new chip was 0.80 even when 0.01 μg of total RNA was used, while it was 0.10 with the reference chip. Additionally, the correlation coefficient between the new and reference DNA chips was 0.88 in the case of 1 μg of total RNA.

These results shows that our DNA chip makes it possible to perform gene expression profiling with only 0.1 μg of total RNA without any amplification. Moreover, it is strongly suggested that our DNA chip has the ability to monitor gene expression profiles even with an amount of total RNA as low as 0.01 μg.

Table 4. **Correlation coefficients of Cy3/Cy5 ratios with different amounts of total RNA.**

Amounts of total RNA (μg)	1 and 0.1	1 and 0.01
New DNA chip	0.87	0.8
Reference DNA chip	0.49	0.1

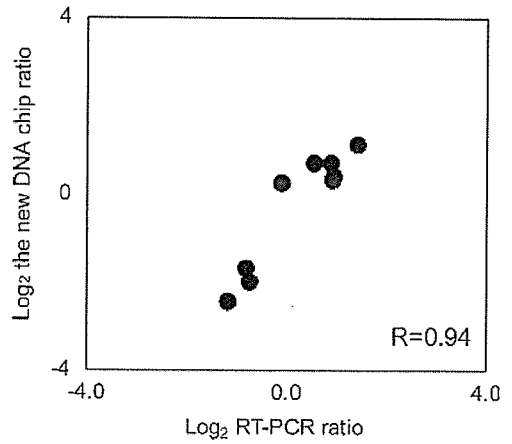

Fig. 6. **Correlation of differential expression ratios (stomach cancer/stomach) for the new DNA chip and RT-PCR (TaqMan).**

To determine the correlation between the signals and the amounts of expressed RNAs, the differential expression ratios obtained with the new DNA chip were compared with those obtained on quantitative real-time PCR analysis. For this analysis, we selected nine genes that are differentially expressed between two human RNA samples (stomach cancer and stomach; BD Bioscience Clontech): HLA-F, PARVB, NR2C1, MDH1, MTI1E, RPL23AP7, BRDT, CD84 and SERPINA1. 5′-Amino-modified 70 bases oligonucleotides originating from the nine genes were chemically synthesized and immobilized on the substrate as described above. The cDNAs hybridized to the new DNA chip were produced from 1 μg of total RNAs. As shown in Fig. 6, the correlation coefficient for both results was 0.94, which is higher than the reported values [0.79–0.92 (*21*)] obtained with a commercially available DNA chip. This result indicates that the new DNA chip can be accurately used to monitor the gene expression ratios in samples.

In this study, we used PMMA as the substrate. PMMA has following the advantages: Firstly, substrates with unique structures can be easily manufactured by means of injection molding. Secondly, it exhibits low autofluorescence. Thirdly, a simple surface modification is available, as shown in Fig. 7b. Although some PMMA surface modification methods have been reported (*22–25*), these methods have a disadvantage, *i.e.*, the PMMA surface tends to be adversely affected by organic solvents or reagents. Here, the question arose as to whether the PMMA substrate contributed to the ultrahigh sensitivity of the new DNA chip. To address this question, the following experiment on the material effect on the sensitivity was carried out. To introduce carboxyl groups onto a glass surface, aminosilane-coated slides (S8111; Matsunami Glass Industries, Ltd.) were immersed in 1-methyl-2-pyrrolidone containing 1.6% (w/v) succinic anhydride (Sigma) and 2.3% (v/v) borate buffer (100 mM, pH 8.0) for 20 min, rinsed with Milli-Q water and then dried (*26*). A 60-mer oligonucleotide composed of a sequence complementary to the target DNA, dissolved in the spotting solution at 30 μM, was spotted robotically and immobilized on glass and PMMA plates with amide binding. The procedures for the reactions are shown in Fig. 7. The target DNA was synthesized from the pKF3 template by the random priming method. The size of the target DNA was estimated to be 200–300 bases on electrophoretic analysis. The hybridization signals on glass and PMMA are shown in Fig. 8, which clearly indicates that the signal intensity on PMMA is superior to that on glass. Although it is not clear why the higher signal intensity was observed in the case of PMMA, we propose

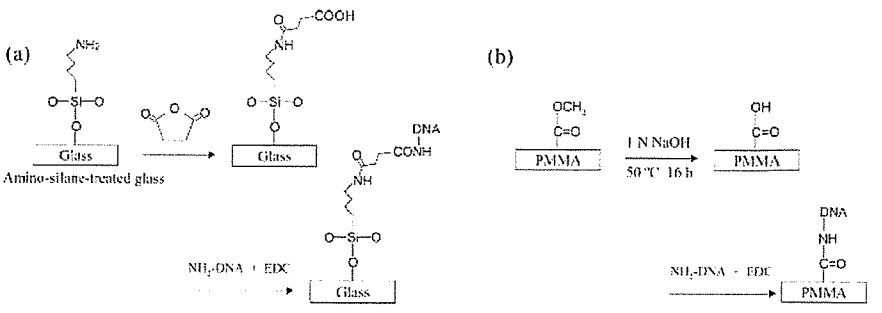

Fig. 7. **Schematic representation of the procedures for immobilization of oligonucleotide on glass (a) and PMMA (b).**

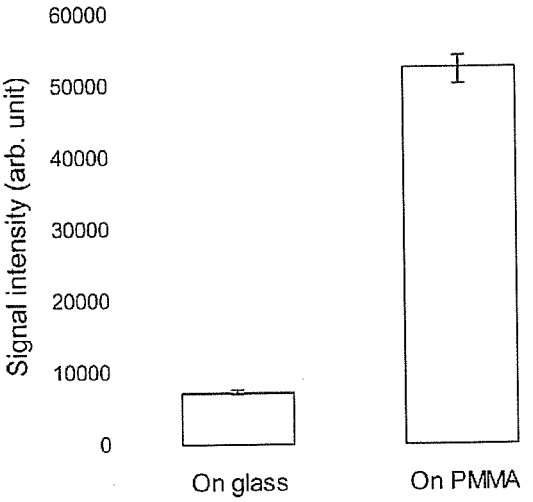

Fig. 8. **Comparison of the hybridization signal intensities of oligonucleotides immobilized on glass and PMMA.** The target DNA was synthesized from the pKF3 template by the random priming method and the oligonucleotide comprised 60 bases.

two possibilities for the signal increase. One possibility is that the PMMA surface might be much rougher than that of glass. Hence, the surface area of a plastic chip might be larger than that of a glass chip. The other possibility is that the influence of steric hindrance might be smaller when a large target DNA hybridizes with an immobilized oligonucleotide on PMMA. When a 20 bases oligonucleotide was immobilized on glass and PMMA plates, and a fluorescent-dye–labeled complementary oligonucleotide (20 bases) was used as the target DNA, interestingly, the signal intensity of PMMA was 0.7–1.2 times as high as that of glass (data not shown). This result implies that a large target DNA can efficiently hybridize with an oligonucleotide on PMMA in comparison with glass. The reason PMMA shows higher hybridization efficiency might be the uneven height of the exposed side chains (carboxyl groups) on PMMA surfaces. This might lead to a lower three-dimensional density of immobilized oligonucleotides on PMMA, resulting in higher hybridization efficiency of a large target DNA.

This work was supported in part by NEDO (New Energy and Industrial Technology Development Organization) through its "Project for Developing Biotechnology IT Integration Equipment."

REFERENCES

1. Flaim, C.J., Chien, S., and Bhatia, S.N. (2005) An extracellular matrix microarray for probing cellular differentiation. *Nature Methods* **2**, 119–125
2. Maekawa, M., Yamamoto, T., Tanoue, T., Yuasa, Y., Chisaka, O., and Nishida, E. (2005) Requirement of the MAP kinase signaling pathways for mouse preimplantation development. *Development* **132**, 1773–1783
3. Soronen, P., Laiti, M., Torn, S., Harkonen, P., Patrikainen, L., Li, Y., Pulkka, A., Kurkela, R., Herrala, A., Kaija, H., Isomaa, V., and Vihko, P.J. (2004) Sex steroid hormone metabolism and prostate cancer. *Biochem. Mol. Biol.* **92**, 281–286
4. Jamshisidi-Parsian, A., Dong, Y., Zheng, X., Zhou H.S., Zacharias, W., and McMasters, K.M. (2005) Gene expression profiling of E2F-1-induced apoptosis. *Gene* **344**, 67–77
5. Zhou, X.J., Kao, M.C., Huang, H., Wong, A., Nunez-Iglesias, J., Primig, M., Aparicio, O.M., Finch. C.E., Morgen, T.E., and Wong, W.H. (2005) Functional annotation and network reconstruction through cross-platform integration of microarray data. *Nature Biotechnol.* **23**, 238–243
6. Katsuma, S., Nishi, K., Tanigawara, K., Ikawa, H., Shiojima, S., Takagaki, K., Kaminishi, Y., Suzuki, Y., Hirasawa, A., Ohgi, T., Yano, H., Murakami, Y., and Tsujimoto, G. (2001) Molecular monitoring of bleomycin-induced pulmonary fibrosis by cDNA microarray-bassed gene expression profiling. *Biochem. Biophys. Res. Commun.* **288**, 747–751
7. Yamada, M., Katsuma, S., Adachi,T., Hirasawa, A., Shiojima, S., Kadowaki, T., Okuno, Y., Koshimizu, T., Fujii, S., Sekiya, Y., Miyamoto, Y., Tamura, M., Yumura, W., Nihei, H., Kobayashi, M., and Tsujimoto, G. (2005) Inhibition of protein kinase CK2 prevents the progression of glomerulonephritis. *Proc. Natl. Acad. Sci. USA* **102**, 7736–7741
8. Van't Veer, L.J., Dai, H., Van de Vijver, M.J., He, Y.D., Hart, A.A.M., Mao, M., Peterse, H.L., Van Der Kooy, K., Marton, M.J., Witteveen, A.T., Schreiber, G.J., Kerkhoven, R.M., Roberts, C., Linsley, P.S., Berarnds, R., and Friend, S.H. (2002) Gene expression profiling predicts clinical outcome of breast cancer. *Nature* **415**, 530–536
9. Gerhold, D.L., Jensen, R.V., and Gullans, S.R. (2002) Better therapeutics through microarrays. *Nature Genetics* **32**, 547–551
10. Margalit, O., Somech, R., Amargio, N., and Rechavi, G. (2005) Microarray-based gene expression profiling of hematologic malignancies: basic concepts and clinical applications. *Blood Rev.* **19**, 223–234
11. Assersohn, L., Gangi, L., Zhao, Y., Dowsett, M., Simon, R., Powles, T.J., and Liu, E.T. (2002) The feasibility of using fine needle aspiration from primary breast cancers for cDNA microarray analyses. *Clin. Cancer Res.* **8**, 794–801
12. Kern, W., Kohlmann, A., Schnittger, S., Hiddemann, W., Schoch, C., and Haherlach, T. (2004) Gene expression profiling as a diagnostic tool in acute myeloid leukemia. *Am. J. Pharmacogenomics* **4**, 225–237
13. Ferrando, A.A. and Look, A.T. (2004) DNA microarrays in the diagnosis and management of acute lymphoblastic leukemia. *Int. J. Hematol.* **80**, 395–400
14. Smith, L., Underhill, P., Pritchard, C., Tymowska-Lalanne, Z., Abdul-Hussein, S., Hilton, H., Winchester, L., Williams, D., Freeman, T., Webb, S., and Greenfield, A. (2003) Single primer amplification (SPA) of cDNA for microarray expression analysis. *Nucleic Acids Res.* **31**, e9
15. Spirin, K.S., Ljubimov, A.V., Castellon, R., Wiedoeft, O., Marano, M., Sheppard, D., Kennet, M.C., and Brown, D.J. (1999) Analysis of gene expression in human bullous keratopathy corneas containing limiting amounts of RNA. *Invest. Ophthalmol. Vis. Sci.* **4**, 3108–3115
16. Wang, E., Miller, L.D., Ohnmacht, G.A., Liu, E.T., and Marincola, F.M. (2000) High-fidelity mRNA amplification for gene profiling. *Nature Biotechnol.* **18**, 457–459
17. Pabon, C., Modrusan, Z., Ruvolo, M.V., Coleman, I.M., Daniel, S., Yue, H., and Arnold, L.J., Jr. (2001) Optimized T7 amplification system for microarray analysis. *Biotechniques* **31**, 874–879
18. Andrej, N.S., Nadine, M., and Richard, I. (2003) Amplified RNA degradation in T7-amplification methods results in biased microarray hybridizations. *BMC Genomics* **4**, 44–57
19. Al-Mulla, F., Al-Tamini, R., and Bitar, M.S. (2004) Comparison of two probe preparation methods using long oligonucleotide microarrays. *Biotechniques* **37**, 827–833
20. Peterlinz, K.A., Georgiadis, R.M., Herne, T.M., and Tarlov, M.J. (1997) Observation of hybridization and dehybridization of Thiol-tethered DNA using two-color surface plasmon resonance spectroscopy. *J. Am. Chem. Soc.* **119**, 3401–3402

21. Shippy, R., Sendera, T., Lockner, R., Palaniappan, C., Kaysser-Kranich, T., Watt, G., and Alsobrook, J. (2004) Performance evaluation of commercial short-oligonucleotide microarrays and the impact of noise in making cross-platform correlations. *BMC Genomics* **5**, 61
22. Henry, A.C., Tutt, T.J., Galloway, M., Davidson, Y.Y., McWhorter, C.S., Soper, S.A., and McCarley, R.L. (2000) Surface modification of poly(methyl methacrylate) used in the fabrication of microanalytical devices. *Anal. Chem.* **72**, 5331–533
23. Waddell, E., Wang, Y., Stryjewski, W., McWhorter, S., Henry, A.C., Evans, D., McCarley, R.L., and Soper, S.A. (2000) High-resolution near-infrared imaging of DNA microarrays with time-resolved acquisition of fluorescence lifetimes. *Anal. Chem.* **72**, 5907–5917
24. Ichijima, H., Kobayashi, M., and Ikada, Y.J. (1992) In vitro evaluation of biocompatibility of surface-modified poly(methyl methacrylate) plate with rabbit lens epithelial cells. *Cataract Refract. Surg.* **18**, 395–401
25. Cheng, J.Y., Cheng, W.W., Hsu, K.H., and Young, H.Y. (2004) Direct-write laser micromachining and universal surface modification of PMMA for device development. *Sensors and Actuators B* **99**, 186–196
26. Hermsndon, T. (1996) *Bioconjugate Techniques*, pp. 90–94, Academic Press, San Diego

High throughput comparative genomic hybridization array analysis of multifocal urothelial cancers

Hiroaki Kawanishi,[1] Takeshi Takahashi,[1] Masaaki Ito,[1] Jun Watanabe,[1] Shin Higashi,[1] Toshiyuki Kamoto,[1] Tomonori Habuchi,[2] Tadashi Kadowaki,[3,4] Gozoh Tsujimoto,[3] Hiroyuki Nishiyama[1] and Osamu Ogawa[1,5]

[1]Department of Urology, Graduate School of Medicine, Kyoto University, 54 Shogoin Kawahara-cho, Sakyo-ku, Kyoto 606-8507; [2]Department of Urology, Akita University School of Medicine, 1-1-1 Hondo, Akita, 010-8543; [3]Department of Genomic Drug Discovery Science, Graduate School of Pharmaceutical Sciences, Kyoto University, 46-29 Yoshida-Shimo-Adachi-cho, Sakyo-ku, Kyoto 606-8501; and [4]Bioinformatics Center, Institute for Chemical Research, Kyoto University, Gokajo, Uji, Kyoto 611-0011, Japan

(Received March 10, 2006/Revised April 18, 2006/Accepted April 24, 2006/Online publication July 6, 2006)

The purpose of this study was to examine genetic alterations occur during synchronous or metachronous multifocal development of urothelial cancers on the whole genome using a comparative genomic hybridization (CGH) array. We used 10 tumor pairs (2 tumors for each patient), in which we had previously defined a clonal relationship by microsatellite analysis. For CGH array analysis, Vysis GenoSensor Array 300 kit was used. An unsupervised hierarchical cluster analysis revealed that the tumors from one patient were clustered together independent of the tumors of all other patients. On the other hand, many genetic divergences among multifocal urothelial cancers were newly found by a CGH array analysis. The concordant genetic alteration patterns of the chromosomal arm in tumor pairs were most frequently observed in 9p, 9q, 8p, 7p, 7q and 11q, while discordant patterns were most frequently found in 15q, 20q, 2q, 10p and 11q. Investigation using a CGH array showed that genetically stable multifocal tumors were less frequent, and that a large percentage of urothelial cancers accumulate genetic alterations during multifocal development by clonal evolution. We might have to consider these genetic accumulations during multifocal development when designing strategies for prevention and detection of recurrent multifocal urothelial cancers. CGH array can be a powerful tool for genetic analysis of multifocal urothelial cancer. (*Cancer Sci* 2006; 97: 746–752)

Urothelial cancers have two clinically important features, multifocality and recurrence. Around 30% of urothelial cancers are found as multiple tumors at the time of diagnosis.[1] Urothelial cancers occur most often (70%) as superficial cancer that can be treated by endoscopic treatment, and 60–80% of patients present one or more recurrences after initial treatment. This multifocal nature of superficial urothelial cancer has been a good material to trace accumulation of genetic alterations in multifocal development of tumor and provided insights into relationship between genetic alterations and carcinogenesis.

Many studies using molecular analysis have suggested a monoclonal origin for multifocal urothelial cancer as appears from X chromosome inactivation studies and genetic and cytogenetic analyzes,[2–5] while other studies have shown an independent origin.[6,7] In our previous LOH analysis of multifocal urothelial cancer using 20 microsatellite markers, we demonstrated that genetic alterations detected were stable in 9 (64%) of the 13 patients with multiple metachronous tumors with a possible identical clonal origin.[5] Because urothelial cancer is characterized by highly complex chromosomal changes affecting numerous chromosomal loci, genome-wide screening may identify genetic divergence among multifocal urothelial cancers that have been missed by the methods applied to date.

Detection of recurrent tumors by non-invasive technique has been an important issue in clinical management of superficial urothelial cancer. Genetic analysis of urine sediments in urothelial cancer patients has been used for diagnosis and follow-up of urothelial cancers, such as FISH, microsatellite analysis and SNP array.[8–11] However, there have been few reports describing the genetic alterations of metachronous multifocal tumors in increased resolution of current technique of DNA analysis.

In this study, to investigate genetic alterations occur during multifocal development of superficial urothelial cancers throughout the genome, we used a Vysis Genosensor CGH array kit with 287 target clone DNAs to analyze 20 tumor specimens from 10 patients in which a clonal relationship had been defined in the previous study using microsatellite analysis.

Materials and Methods

Patients and tumor samples

Topologically distinct urothelial cancers of the bladder, ureter, and renal pelvis in 10 patients were included in this study (2 tumors for each patient). Tumor samples were snap-frozen and stored –80°C until DNA extraction. The present study did not include tumor materials which contaminated more than 20% of

[5]To whom correspondence should be addressed, E-mail: ogawao@kuhp.kyoto-u.ac.jp
Abbreviations: BAC, bacterial artificial chromosome; CGH, comparative genomic hybridization; DAPI, 4,6,-diamidino-2-phenylindole; dCTP, 2'-deoxycytidine 5'-triphosphate; FISH, fluorescence *in situ* hybridization; LOH, loss of heterozygosity; PAC, P1-derived artificial chromosome; PCR, Polymerase Chain Reaction; SNP, single nucleotide polymorphisms; WHO, world health organization; SSC, sodium chrolide-sodium citrate.

doi: 10.1111/j.1349-7006.2006.00259.x

Table 1. Characteristics of 20 multifocal urothelial tumors of 10 patients

Patient		Tumor	Interval (month)	Site†	Grade	pT
Group I	9	2		B2	1	a
		8	38	B4	1	a
	26	1		B5	2	1
		2	0	B2	2	1
	2	2		B3	1 > 2	a
		8	3	P	1,2	a
	18	1		B2	1	a
		2	12	B2	1	a
	10	1		P	2	1
		2	7	B2	2	1
	15	1		B2	2	1
		2	37	B2	2	1
Group II	21	1		B1	2	1
		5	8	B2	2 > 1	a
	16	1		U	2	a
		4	7	B2	2	NE‡
	23	1		P	2	3
		2	18	B4	2	a
	30	1		B2	2	a
		2	8	B5	2	a

Patients were divided into two groups by the previous microsatellite analysis.[5] Group I patients had concordant LOH patterns alone. Group II patients had both discordant and concordant LOH patterns. †U, ureteral tumor; P, renal pelvic tumor; B, bladder tumor [the locations of the bladder tumor were as follows: B1, trigone; B2, posterior wall; B3, right wall; B4, left wall, B5, dome]; ‡NE, not examined.

normal interstitial cells in hematoxylin and eosin (HE) staining. Normal reference DNA was obtained from the peripheral blood of each patient. Tumor and reference DNAs were prepared by proteinase K digestion and phenol/chloroform extraction. The tumor stage and grade were classified according to the tumor-node-metastasis system and WHO criteria, respectively,[12,13] by pathologists who were unaware of the aims of this study. All tumors were urothelial carcinomas, and brief clinical and pathological data are presented in Table 1.

These specimens were analyzed in our previous LOH study and a clonal relationship had already been defined.[5] Using microsatellite markers, we examined genetic alterations at 20 loci on eight chromosome arms (2q, 4p, 4q, 8p, 9p, 9q, 11p, and 17p). The markers we used D2S206 and D2S336 on chromosome 2q; D4S404 and D4S1546 on 4p; D4S426 and D4S171 on 4q; D8S261 and D8S520 on 8p, D9S171, D9S126, D9S1749 and D9S736 on 9p; D9S66, D9S1848, D9S1793 and GSN on 9q, D11S907 and D11S922 on 11p; and D17S796 and D17S1176 on 17p. Completely identical LOH patterns were detected in six patients (No. 9, 26, 2, 18, 10, and 15), while discordant patterns together with concordant patterns were observed in the remaining four patients (No. 21, 16, 23, and 30). In patient 30, no clonal relationships could be defined in the previous microsatellite study. All tumor pairs in other patients were considered to be monoclonal based on the results of microsatellite analysis. Written informed consent was obtained from each patient before surgery, according to the ethical guidelines of our university.

Array-based CGH (Array CGH)

Array-based CGH was performed using a GenoSensor Array 300 kit (Vysis, Downers Grove, IL), which contained 287 target clone DNAs (P1, PAC or BAC clones) representing regions that are important in cytogenetics and oncology. Each DNA clone was arrayed on the slide in three spots. Tumor and reference DNAs (100 ng) were labeled with Cy3-dCTP or Cy5-dCTP (Perkin Elmer, Wellesley, MA), respectively, by random priming reaction. Labeled DNAs were mixed with a microarray hybridization buffer that contained a high concentration of Cot-1 DNA (Vysis). The probe mixture was denatured at 80°C for 10 min and incubated at 37°C for 1 h before being transferred to the microarray. After an overnight hybridization at 37°C, the microarrays were washed three times with 50% formamide/2XSSC at 40°C for 10 min each. Thereafter, the microarrays were subjected to four washes with 1XSSC at room temperature for 5 min each. The microarrays were counterstained with the DAPI IV mounting solution (Vysis).

Images of fluorescence signals were captured and analyzed with the GenoSensor Reader System and GenoSensor Reader software (Vysis) according to the manufacturer's instructions. The mean normalized test/reference (T/R) ratio was calculated from each set of T/R ratio of three spots. Gain and loss of DNA copy number were judged by T/R ratios >1.2 and <0.8, respectively. Two different sets of labeling and hybridization tests were performed on two tumors from one patient (Patient No. 15) to validate the reproducibility of the GenoSensor Array 300 kit. Spots on which the difference in the ratios was greater 0.2 were 3 (1%) of 286 evaluated spots in tumor 1 and 1 of 286 (0.3%) in tumor 2.

Data analysis of array CGH Results

We performed an unsupervised hierarchical cluster analysis on log base 2 transformed data obtained for 287 target clones to weight how the prevalence of genomic changes is similar or different. The Ward linkage and cosine coefficient metric were used. The results were visualized in the software program R.

In order to assess global chromosomal aberrations in multifocal urothelial cancers, our subsequent analysis focused to 'the pattern of chromosomal aberrations between tumor pairs in each patient'. On one clone of the array, an identical genetic alteration of two tumors in one patient was defined when a loss or gain was detected and the result was identical. Different genetic alterations were defined as follows: 1. Loss or gain was detected; 2. The result was different in the two tumors; 3. The difference in the ratio of the two tumors was greater than 0.2. Then, the pattern of chromosomal aberrations compared between tumor pairs was evaluated on each chromosomal arm. The pattern of chromosomal aberrations was defined as concordant or discordant if identical or different gains or losses were detected in 2 or more clones on the chromosomal arm. If both discordant and concordant patterns coexisted, we defined the chromosomal arm as discordant. A chromosomal arm which had only one clone with a gain or loss was neglected.

Quantitative real-time PCR

Quantitative real-time PCR analyzes were performed on the same set of urothelial cancers to detect copy number changes for four genes, *BIN1* (2q14), *CDKN2A (p16)* (9p21), *CCND1*

(11q13), and *MAP2K5* (15q23), which were included in the CGH array target DNAs. The relative gene copy number was evaluated by the comparative C_T Method as described by Ginzinger *et al.*[14] on the ABI Prism 5700 Sequence Detection System (PE Applied Biosystems, Foster City, CA). The *PFKL* gene served as an internal control, located on 21q22.3, which is rarely altered numerically in urothelial cancers.[15] Twenty normal peripheral blood samples were examined to determine the reference range.

Results

Overall results

Of 287 clones examined in 20 tumors (5740 in total) gain and loss were observed in 437 (7.6%) and 512 (8.9%), respectively. On average, one tumor had gains in 21.9 (4–42) clones and losses in 25.6 (1–53) clones. The identical alterations between tumor pairs were most frequently observed in CDKN2A (p16) (9p21), MTAP (9p21.3), and AFM137XA11 (9p11.2) (6 patients), CTSB (8p22), D8S596 (8p Tel.), D8S504 (8p Tel.), AF170276 (9p Tel.) and D9S913 (9p Tel.) (5 patients). On the other hand, the different alterations between tumor pairs were frequently identified in SNRPN (15q12), UBE3A, D15S10 (15q11-q13) and STK6 (20q13.2-q13.3) (4 patients), MYBL2 (20q13.1) and PTPN1 (20q13.1-q13.2) (3 patients). These genes/loci may be susceptible to genetic alterations during multifocal development of urothelial cancers.

Hierarchical clustering analysis

Fig. 1 shows the cluster dendrogram of 20 tumors of 10 patients based on the similarity of genetic alterations detected by CGH array analysis. Tumor pairs from one patient were clustered together. One tumor was more related to the second tumor from the same patient than tumors from all other patients, suggesting that these tumor pairs were clonally related.

The pattern of chromosomal aberrations on the CGH array

On average, concordant patterns of chromosomal aberrations were detected in 5.8 chromosomal arms (range 1–13) in one patient; while discordant patterns were detected in 4.2 chromosomal arms (range 0–12). Fig. 2 summarizes the patterns of chromosomal aberrations.

In 8 of 10 patients, both concordant and discordant patterns were observed. In patient No. 9, concordant patterns were found in chromosomal arms 8q (gain), 9p (loss), 11p (partial loss), 12q (partial gain) and 22q (partial loss), while discordant patterns were found in 1p, 2p, 8p, 9q, 18p and 18q (Fig. 3a,b). In 2 of

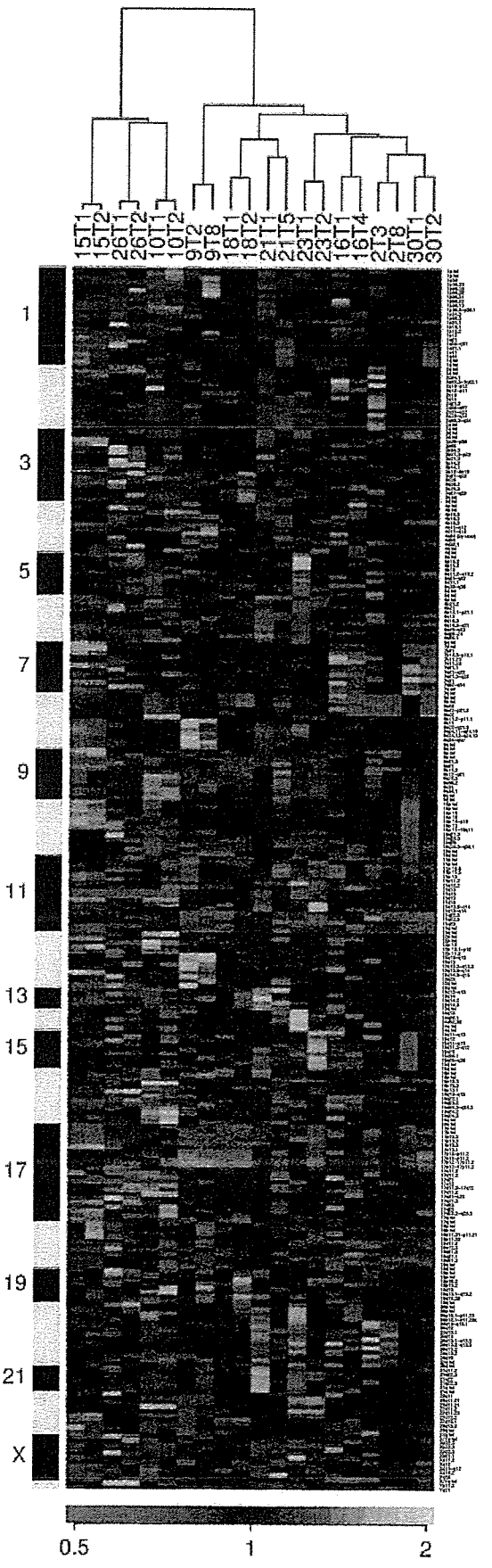

Fig. 1. Hierarchical clustering of data from 287 clones on the GenoSensor array 300 in 20 tumors. The data are presented in a matrix format. A column corresponds to a single tumor, and each row corresponds to a single clone ordered by mapping position. Gain or loss of a clone is represented by the color of the corresponding cell in the matrix. Green indicates gain; black, no change; and red, loss. Color saturation is proportional to the magnitude of the difference. The sidebars to the left of the matrix format represent chromosome cluster, ordered from chromosome 1 to Y. The horizontal dendrogram shows the association between the tumors and the length of the branches of the dendrogram reflects the similarity between tumors. Note that one tumor is more related to the second tumor from the same patient than tumors from all other patients.

doi: 10.1111/j.1349-7006.2006.00259.x

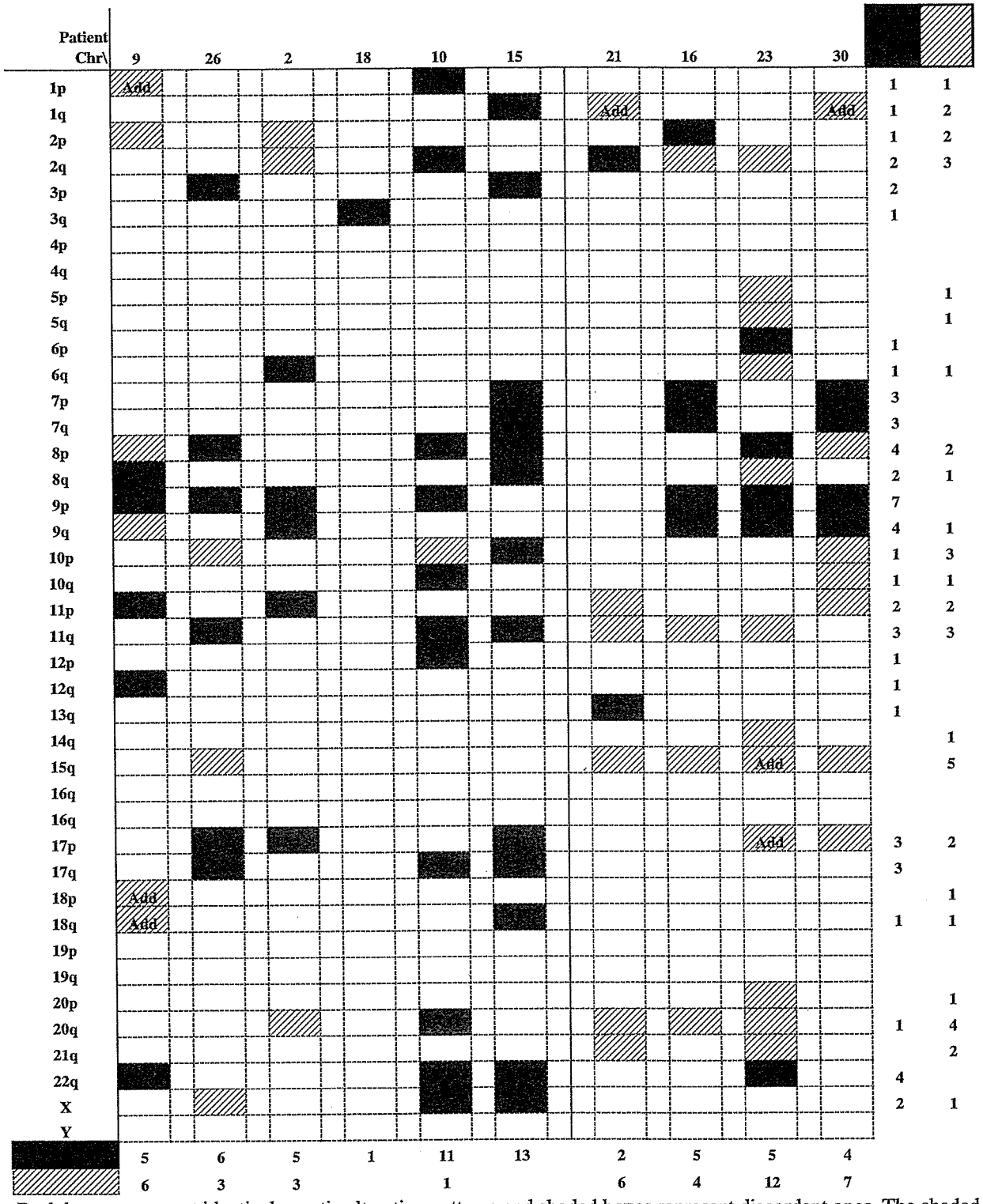

Dark boxes represent identical genetic alteration patterns and shaded boxes represent discordant ones. The shaded boxes with 'Add' represent simple addition of genetic alteration, which means latter tumor had additional genetic alteration to that of former tumor. The shaded boxes without 'Add' represent genetic diversity, which means that former tumor has discordant genetic alterations which latter tumor does not.

Fig. 2. Summary of genetic alteration patterns of chromosomal arms.

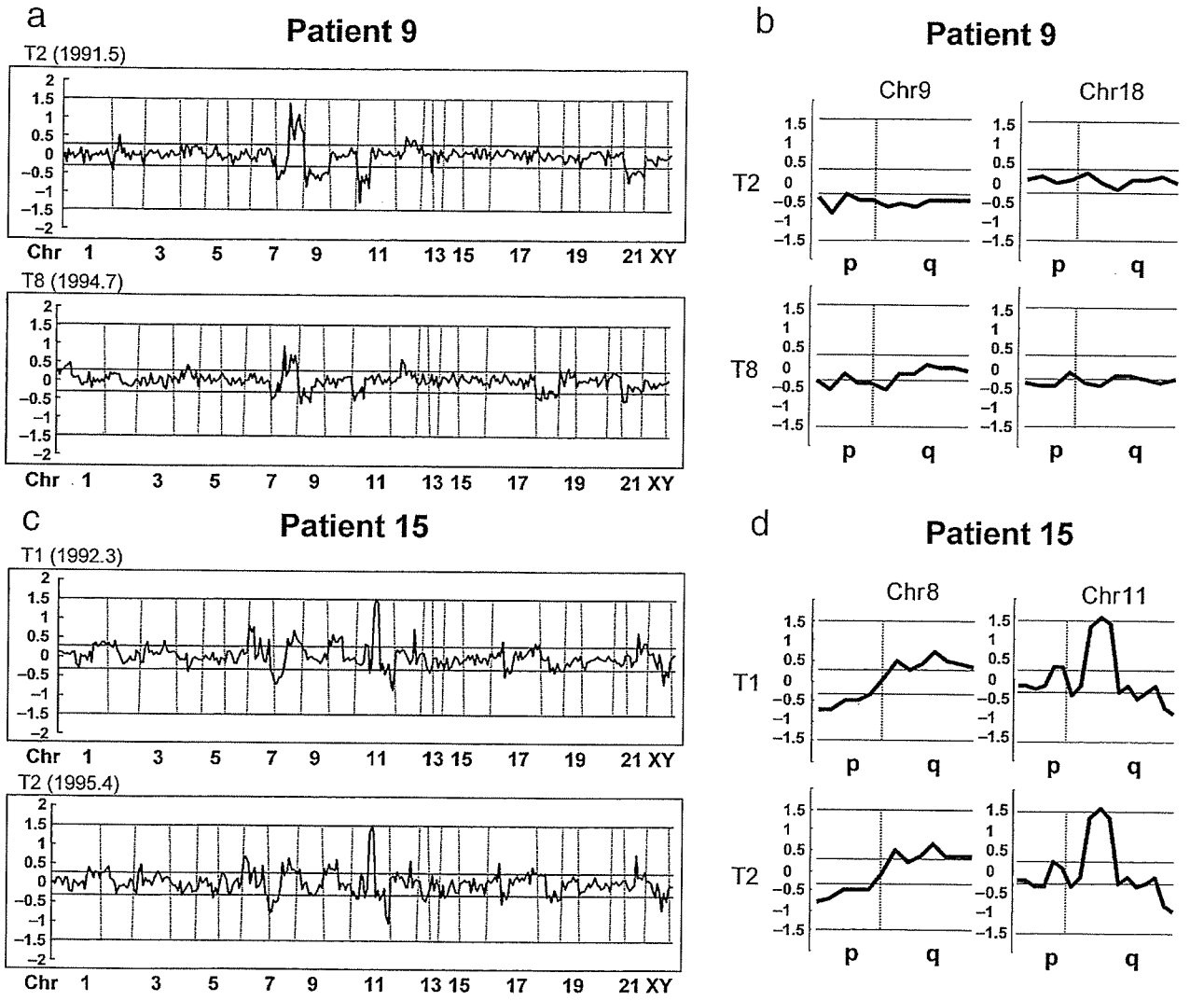

Fig. 3. (a,c) Graphical representation of CGH array analysis of patient No. 9 and 15, whole genome. Vertical lines indicate the boundaries of chromosomes. Both concordant and discordant patterns of chromosomal aberrations were observed in patient No. 9, while the patterns of chromosomal aberrations were completely identical in patient No. 15. (b,d) Representative chromosome arms. In patient No. 9, a concordant pattern was found in 9p (loss), while discordant patterns were found in 9q, 18p and 18q. In patient No. 15, loss of 8q, gain of 8q, and a partial loss and gain of 11q were observed in both tumors. Vertical lines indicate boundaries of chromosome arms. Average $\log_2$ ratios were plotted for all clones on chromosome position. Thresholds for gain or loss are shown within $\log_2$ ratios of 0.2 and −0.2, respectively. T; tumor, Chr; chromosome.

10 patients, the patterns of chromosomal aberrations were identical. The results of patient No. 15 are shown in Fig. 3c,d. Of note, these two tumors developed with a 3 years interval and the patient had 4 tumor recurrences between the two tumors. These data suggest that in part of superficial bladder cancers, the whole genome is genetically stable during development of metachronous cancers.

Concordant patterns of chromosomal aberrations between tumor pairs were most frequently observed in 9p (7 patients), 8p (5 patients), 9q, 22q (4 patients), 7p, 7q, 11q, 17p and 17q (3 patients). Among concordant patterns, aberrations on 9p, 9q, 8p and 17p were losses of the chromosomal arm, and on 7p, 7q and 17q were gains. Discordant patterns were most frequently found in 15q (5 patients), 20q (4 patients), 2q, 10p, and 11q (3 patients). Among the total 42 discordant patterns, simple addition of genetic alterations to latter tumor was found in only 7, which suggests that the accumulation of genetic alterations does not parallel the chronological order of tumor occurrence.

Comparison of CGH array and PCR-based microsatellite analysis

Exactly same loci to 20 microsatellite markers used in the previous study were not included in the CGH array target DNAs. Of 20 microsatellite markers used in the previous study, 6 markers for which the distance to the nearest spot on the CGH array was within 1 Mb length were selected and the results of the 2 methods were compared. Of 104 informative microsatellite analyzes using 6 markers, D8S520, D9S126, D9S1749, D9S1848, D9S66 and D11S922, 61 showed

doi: 10.1111/j.1349-7006.2006.00259.x

LOH. Overall, of 104 informative microsatellite analyzes, 59 (56.7%) matched the results of the CGH array. Among the 61 LOH, 36 (59%) were detected as gains or losses by the CGH array. The results of the CGH array analysis and microsatellite analysis were not closely matched, probably it is because the loci of most microsatellite markers were not exactly same as those of the spot on the CGH array. In addition, the difference in the result may be caused by the difference of the assay platform; microsatellite involves amplification step while the CGH array does not.

Validation of CGH array analysis by quantitative Real-time PCR

Quantitative real-time PCR was performed on all tumor samples using four genes. We calculated the Pearson correlation coefficient (r) between the results of the CGH analysis and quantitative real-time PCR analysis. We found a strong correlation BINI ($r = 0.75$), CDKN2A ($r = 0.70$), CCND1 ($r = 0.96$), and MAP2K5 ($r = 0.71$) between them. Both methods matched in 87.5% (70 of 80) when the copy numbers of each gene/locus were decided by using their respective cutoff criteria. The discordant results between them were found only in the case which the genes/loci had the subtle copy number gain/loss. The discordance of the results using both methods may be inevitable to some degree in cases of subtle copy number gain/loss. In addition, the difference in the result is probably caused by the difference of assay methodology, or the low resolution of the CGH array. Among 7 tumor pairs showing a discordant pattern of chromosomal aberrations in the CGH array, we also obtained matched results in 4 pairs in quantitative real-time PCR analysis.

Discussion

In the present study, using commercially available CGH array kits, we investigated global chromosomal aberrations in multifocal urothelial cancers. The multiloci survey by the CGH array of the whole genome enabled us to detect genetic alterations on the loci that we did not detect in the previous study. In the previous report, 64% of tumor pairs showed completely identical LOH patterns and we concluded that a high percentage of superficial urothelial cancers are genetically stable. However, among tumor pairs of 6 patients with completely concordant LOH patterns on microsatellite analysis, discordant patterns of chromosomal aberrations between tumor pairs were newly found in 4 patients using the CGH array. The current results showed that such genetically stable multifocal cancers are rather infrequent and that a large number of superficial urothelial cancers accumulate genetic alterations during multifocal development. On the other hand, in patients 18 and 15, only concordant chromosomal aberration patterns were observed even by genome-wide CGH array analysis, which indicates that some multifocal urothelial cancers are genetically stable during multifocal development.

Since the introduction of molecular analysis into clonal analysis, the majority of multifocal urothelial cancers have been suggested to be monoclonal or have a common clonal origin.[4,16,17] In multistep carcinogenesis model, an original transformed cell grows out and sheds cells into the lumen of the bladder. Some of these cells will have required additional genetic alterations. Interestingly, among the 42 discordant patterns, simple addition of genetic alterations to latter tumor was found in only 7. In these tumor pairs, the latter tumor is not directly derived from the former tumor. van Tilborg *et al.* performed the LOH analysis of metachronous multifocal bladder cancer using 48 microsatellite markers,[18] and reported similar findings to our data. To develop a strategy to prevent and detect recurrent multifocal urothelial cancers, it should be remembered that the chronology of tumor appearance does not always run in parallel with the accumulation of genetic alterations during the process of intraepithelial spread or intraluminal seeding. The commercially available CGH array used in this study is a relatively low-resolution scan, and much higher resolution scans of the bladder cancer genome have been reported.[19] By using a CGH array with high resolution and high throughput for analysis of a larger number of samples, we might be able to draw more detailed genetic trees and pedigrees of multifocal urothelial cancers and trace genetic alterations accumulated during multifocal development.

The development and progression of urothelial cancer is the result of a series of genome instability occurring over the lifetime of a tumor. The number of chromosomal alterations was reported to be higher in high grade, advanced stage tumors.[20,21] Discordant chromosomal aberrations between multifocal tumors might reflect genome instability as well. It would be useful to know whether the degree of discordant chromosomal aberrations has an association with recurrence, progression, tumor grade and stage. Considering that most tumors we analyzed were low grade superficial type, it is likely that many of the chromosomal aberrations we detected were not related to differences in grade or stage. With accumulation of data on the chromosomal aberrations of multifocal tumors, it might become possible to identify target chromosomal regions and target genes which play an important role in recurrence, progression and invasion of urothelial cancers.

A number of studies have reported the detection of tumor cells in urine. Halling *et al.* reported high sensitivity (81%) of multicolor FISH analysis consisting of probes for chromosome 3, 7 and 17, and the 9p21 band in detecting urothelial cancer.[8] Several investigators showed that 85% or greater sensitivity was achieved using 13–20 highly informative microsatellite markers to detect genetic alterations in urinary exfoliated cells.[9,10] Furthermore, Hoque *et al.* used a SNP array to detect urothelial cancer and reported a 100% detection rate.[11] Our data suggest that we should be careful when we use these genetic methods for monitoring urothelial cancer recurrence, because the genetic alterations we detect in primary tumors may not be present in recurrent tumors. In the current study, concordant patterns of chromosomal aberrations were frequently detected on 9p, 8p, 9q, 22q, 7p, 7q, 11q, 17p and 17q. The loci on these chromosomal arms may be good candidates for probes for efficient monitoring of urothelial cancer recurrence. Furthermore, our data is consistent with the view that genetic alterations on chromosome 9 occur early in the development of multifocal urothelial cancer and remain stable during clonal progression. Accumulation of data regarding chromosomal aberrations among multifocal urothelial cancers would be necessary to improve efficiency and reduce the cost of the genetic analysis to detect tumor cells in urinary exfoliated cells.

References

1 Kiemeney LA, Witjes JA, Heijbroek RP, Verbeek AL, Debruyne FM. Predictability of recurrent and progressive disease in individual patients with primary superficial bladder cancer. *J Urol* 1993; **150**: 60–4.
2 Sidransky D, Frost P, Von Eschenbach A, Oyasu R, Preisinger AC, Vogelstein B. Clonal origin bladder cancer. *N Engl J Med* 1992; **326**: 737–40.
3 Habuchi T, Takahashi R, Yamada H, Kakehi Y, Sugiyama T, Yoshida O. Metachronous multifocal development of urothelial cancers by intraluminal seeding. *Lancet* 1993; **342**: 1087–8.
4 Dalbagni G, Ren ZP, Herr H, Cordon-Cardo C, Reuter V. Genetic alterations in tp53 in recurrent urothelial cancer: a longitudinal study. *Clin Cancer Res* 2001; **7**: 2797–801.
5 Takahashi T, Habuchi T, Kakehi Y *et al.* Clonal and chronological genetic analysis of multifocal cancers of the bladder and upper urinary tract. *Cancer Res* 1998; **58**: 5835–41.
6 Miyake H, Hara I, Kamidono S, Eto H. Multifocal transitional cell carcinoma of the bladder and upper urinary tract: molecular screening of clonal origin by characterizing CD44 alternative splicing patterns. *J Urol* 2004; **172**: 1127–9.
7 Jones TD, Wang M, Eble JN *et al.* Molecular evidence supporting field effect in urothelial carcinogenesis. *Clin Cancer Res* 2005; **11**: 6512–19.
8 Halling KC, King W, Sokolova IA *et al.* A comparison of BTA stat, hemoglobin dipstick, telomerase and Vysis UroVysion assays for the detection of urothelial carcinoma in urine. *J Urol* 2002; **167**: 2001–6.
9 Steiner G, Schoenberg MP, Linn JF, Mao L, Sidransky D. Detection of bladder cancer recurrence by microsatellite analysis of urine. *Nat Med* 1997; **3**: 621–4.
10 Schneider A, Borgnat S, Lang H *et al.* Evaluation of microsatellite analysis in urine sediment for diagnosis of bladder cancer. *Cancer Res* 2000; **60**: 4617–22.
11 Hoque MO, Lee J, Begum S *et al.* High-throughput molecular analysis of urine sediment for the detection of bladder cancer by high-density single-nucleotide polymorphism array. *Cancer Res* 2003; **63**: 5723–6.
12 Sobin LH, Wittekind Ch. *UICC TNM Classification of Malignant Tumours*, 5th edn. New York: John Wiley & Sons, Inc. 1997.
13 Fleming ID, Cooper JS. *Henson DE et al. American Joint Committee on Cancer on Cancer Staging Manual*, 5th edn. Philadelphia: JB Lippincott 1997.
14 Ginzinger DG, Godfrey TE, Nigro J *et al.* Measurement of DNA copy number at microsatellite loci using quantitative PCR analysis. *Cancer Res* 2000; **60**: 5405–9.
15 Aveyard JS, Knowles MA. Measurement of relative copy number of CDKN2A/ARF and CDKN2B in bladder cancer by real-time quantitative PCR and multiplex ligation-dependent probe amplification. *J Mol Diagn* 2004; **6**: 356–65.
16 Hafner C, Knuechel R, Stoehr R, Hartmann A. Clonality of multifocal urothelial carcinomas: 10 years of molecular genetic studies. *Int J Cancer* 2002; **101**: 1–6.
17 Simon R, Eltze E, Schafer KL *et al.* Cytogenetic analysis of multifocal bladder cancer supports a monoclonal origin and intraepithelial spread of tumor cells. *Cancer Res* 2001; **61**: 355–62.
18 van Tilborg AA, de Vries A, de Bont M, Groenfeld LE, van der Kwast TH, Zwarthoff EC. Molecular evolution of multiple recurrent cancers of the bladder. *Hum Mol Genet* 2000; **9**: 2973–80.
19 Veltman JA, Fridlyand J, Pejavar S *et al.* Array-based comparative genomic hybridization for genome-wide screening of DNA copy number in bladder tumors. *Cancer Res* 2003; **63**: 2872–80.
20 Primdahl H, Wikman FP, von der Maase H, Zhou XG, Wolf H, Orntoft TF. Allelic imbalances in human bladder cancer: genome-wide detection with high-density single-nucleotide polymorphism arrays. *J Natl Cancer Inst* 2002; **94**: 216–23.
21 Hoque MO, Lee CC, Cairns P, Schoenberg M, Sidransky D. Genome-wide genetic characterization of bladder cancer. a comparison of high-density single-nucleotide polymorphism arrays and PCR-based microsatellite analysis. *Cancer Res* 2003; **63**: 2216–22.

doi: 10.1111/j.1349-7006.2006.00259.x